

Dynamics of Non-superconducting Pairs in $\text{YBa}_2\text{Cu}_3\text{O}_{7-\delta}$ Below T_c

Jinzhong Zhang¹, Xinhang Cai¹, Qingming Huang¹, Yihong Chen¹, Zhangqiang Yang¹, Zhiyuan Sun², Ye Yang^{1,3}

1. State Key Laboratory of Physical Chemistry of Solid Surfaces, College of Chemistry and Chemical Engineering, Xiamen University, Xiamen 361005, China
2. Department of Physics, Tsinghua University, Beijing 100084, China
3. Innovation Laboratory for Sciences and Technologies of Energy Materials of Fujian Province (IKKEM), Xiamen 361005, China

Abstract: Pairing states are essential for understanding the underlying mechanisms of high-temperature superconductivity. Here the non-superconducting state in an optimally doped $\text{YBa}_2\text{Cu}_3\text{O}_{7-\delta}$ film was driven out of equilibrium by an optical pump with low fluence at a temperature well below the critical temperature (T_c), and its recovery dynamics were exclusively measured using transient terahertz spectroscopy. The pump-fluence dependent experiments unveiled evidence of local pairs without superconductivity coexisting with the superconducting Cooper pairs. An energy gap opening induced by the local pairing with short-range coherence was invoked to rationalize the temperature-dependent recovery time of local pairs with a characteristic divergence at a temperature substantially below T_c . These local pairs displayed remarkable likeness to the short-range pair-density-wave state. Our finding shed light on understanding the dynamic interplay between the coexisting superconducting and non-superconducting pairs in cuprate superconductors.

Cuprate superconductors exhibit critical temperatures significantly higher than conventional superconductors, which has spurred extensive research into understanding their underlying mechanisms. One of the central questions revolves around the pairing mechanism responsible for the formation of Cooper pairs, which is fundamentally different from the pairing in conventional superconductors described by Bardeen-Cooper-Schrieffer (BCS) theory.[1] The Cooper pairs can condense into a superfluid with long-range coherence and thus give rise to superconductivity. In conventional BCS superconductors, the formation of Cooper pairs and the establishment of long-range coherence occur simultaneously below the critical temperature (T_c). However, these two quantum phenomena take place separately in the cuprate (particularly in the underdoped ones) and other unconventional SCs.[2-7] In these superconductors, pairing may also lead to Cooper pairs without superconductivity, i.e., without long-range phase coherence. It has been demonstrated that

electron pairs preform at temperatures above T_c via local pairing, which might account for the opening of a pseudogap.[2,8] At a temperature well below T_c , signatures of local pairs without long-range coherence have also been observed using scanning tunneling microscopy,[9-12] and the charge order revealed by this technique is conjectured to be intimately related to a short-range pair-density-wave (PDW) state coexisting with the d-wave superconductivity.[13-18] However, it is very challenging to measure the interplay between superconducting pairs and local pairs below T_c using the steady state experimental tools because a fine balance is established between them in thermal equilibrium. Inspired by the time-resolved spectroscopic studies on superconductors, the recovery dynamics from a light-induced nonequilibrium state can provide insights into the interplay between the coexisting states. [19-41]

Since the superconducting and non-superconducting states exhibit distinct frequency-dependent complex conductivities, the transient terahertz (THz) spectroscopy can be exploited to separately track their respective restoration dynamics after optical excitation. Here, using this technique, we uncovered the pairwise recombination of nonequilibrium quasiparticles in an optimally doped $\text{YBa}_2\text{Cu}_3\text{O}_{7-\delta}$ (YBCO) film. At temperature well below T_c , the transient THz response for low pump fluence primarily arises from the partial depletion of the non-superconducting state whose recovery proceeds in a pairwise fashion, indicative of the existence of local pairs at the ground state. The mobility of these local pairs is remarkably greater than the photoinduced nonequilibrium quasiparticles. The temperature dependence of the time constant for the recovery of the non-superconducting state shows a clear divergence near 70 K (notably below the T_c), which is reminiscent of the recovery of the superconducting state except that its recovery time diverges near T_c . Like the superconducting energy gap, an energy gap opening associated with local pairing is likely manifested as a divergence of the non-superconducting state recovery time. Our findings provide evidence of local pairs that display remarkable likeness to the short-range PDW state that coexists with the superconducting state.

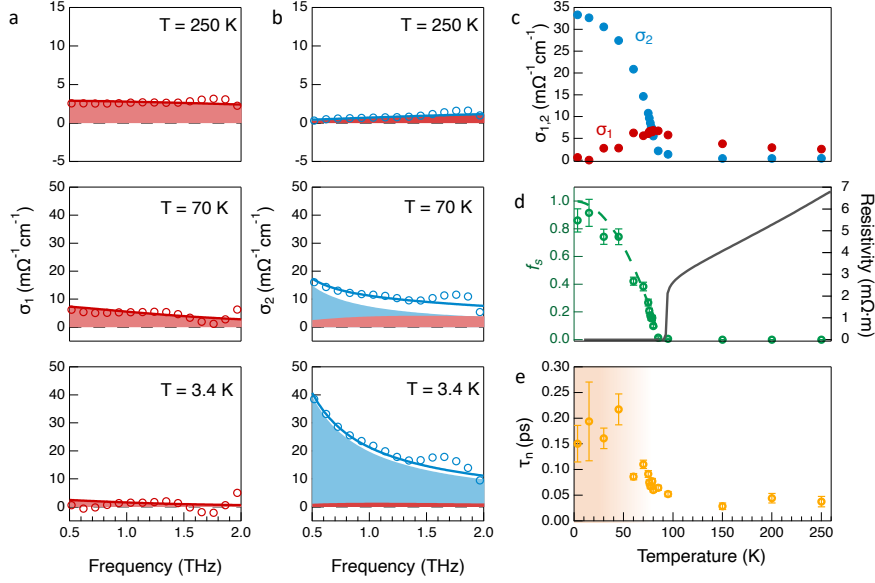


Figure 1. Temperature dependence of terahertz conductivities at equilibrium condition. (a) Real (σ_1) and (b) imaginary (σ_2) parts of the YBCO steady state conductivity of measured at typical temperatures (symbols). Solid curves represent the two-fluid model. The red and blue shades represent the Drude and superfluid contributions, respectively. (c) Temperature dependence of σ_1 and σ_2 magnitudes recorded at 0.6 THz. (d) The measured (green circles) and calculated (green dash curve) superfluid fraction, f_s , at various temperatures. The black solid curve shows the electric resistivity as function of temperature. (e) Temperature dependent scattering time of the normal conducting carriers.

The $\text{YBa}_2\text{Cu}_3\text{O}_{7-\delta}$ ($\delta \approx 0.1$) thin film was deposited on a MgO substrate using magnetron sputtering, and the critical temperature for this sample is determined to be 91 K (Fig. S1). The complex conductivities ($\tilde{\sigma}$) of the YBCO film over the frequency range of 0.5 to 2.0 THz were measured using the steady-state THz spectroscopy at various temperatures (Fig. S2). At a temperature well above T_c (e.g., $T = 250$ K), the real and imaginary parts of $\tilde{\sigma}$, denoted as σ_1 and σ_2 , respectively, show typical Drude responses, characteristic of metallic conductivity (Fig. 1a and 1b). As the temperature drops below T_c , σ_1 is fading away because the spectral weight tends to condense into the delta function at zero frequency, while σ_2 shows a spectral weight transfer from the high frequency to the low frequency. For $T \ll T_c$ (e.g., $T = 3.4$ K), σ_2 displays a typical $1/\omega$ dependence, a hallmark of superconductivity. The temperature dependence of $\tilde{\sigma}$ for YBCO observed here aligns well with the literature,^[42-46] which can be described by the phenomenological two-fluid model. In this model, $\tilde{\sigma}$

consists of two components: a superfluid component from the condensed Cooper pairs and a Drude component from the non-superconducting quasiparticles, which is expressed as

$$\tilde{\sigma}(T) = \rho_n(T) \frac{\tau_n(T)}{1 - i\omega\tau_n(T)} + \rho_s(T) \frac{i}{\omega} \quad (1)$$

where $\rho_n(T)$ and $\rho_s(T)$ are the effective densities of non-superconducting and superconducting carriers, respectively, and τ_n is the scattering time for the non-superconducting carriers. The sum of $\rho_n(T)$ and $\rho_s(T)$ is constrained by the total number of electrons and assumed to be constant as temperature varies, and the fraction of superconducting carriers, $f_s(T)$, is then defined as $\rho_s(T) / [\rho_s(T) + \rho_n(T)]$. By substituting this expression into Eq. (1), the temperature dependence of $\tilde{\sigma}$ is found to be governed by the temperature-dependent $f_s(T)$ and $\tau_n(T)$, which are then set as free fitting parameters. The fitting curves (solid curves, Fig. 1a and 1b) excellently match the experimental data (symbols, Fig. 1a and 1b). This model indicates that below T_c , σ_1 comprises the pure Drude component, while σ_2 consists of both superfluid (blue shades, Fig. 1b) and Drude (red shades, Fig. 1b) contributions. The two-fluid model was also successfully applied to $\tilde{\sigma}$ at other temperatures (Fig. S2).

The temperature dependent magnitudes of σ_1 and σ_2 display dramatic changes near T_c (Fig. 1c), consistent with the literature.[43,45-48] More specifically, σ_2 rises steeply when temperature drops below T_c due to the growing superfluid density. In comparison, σ_1 first increases and then decreases with decreasing temperature, leading to a peak near T_c . It is worth noting that σ_1 does not extinct even when temperature drops far below T_c , indicative of a small residual Drude component. The onset of the temperature dependent $f_s(T)$ extracted from the fitting corresponds to the beginning of condensation, i.e., T_c , which coincides with that determined from temperature dependent electric resistivity (Fig. 1d). This consistence also validates the THz spectroscopic method for detecting superconductivity. The temperature dependence of $f_s(T)$ basically obeys the relation $f_s(T) = 1 - (T/T_c)^2$ (green dash curve, Fig. 1e), which is typical for a dirty d-wave superconductor.[45,48,49] Nonetheless, the measured f_s deviates from the calculation as the temperature approaches zero (i.e., f_s is smaller than the calculated value). Both the residual σ_1 (Fig. 1c) and less-than-unity f_s (Fig. 1d) at 3.4 K confirm that a small fraction of carriers remains non-superconducting although the superfluid condensate prevails, which evidences the coexistence of superconducting and non-superconducting carriers at this temperature. The temperature dependent

τ_n given by the fitting is displayed in Fig. 1e. Despite the large fitting uncertainties, we can still discern an abrupt change at approximately 70 K where $\tau_n(T)$ rises steeply, a sign of a possible phase transition for the non-superconducting carriers. An abrupt increase of τ_n at temperature below T_c was also observed by microwave spectroscopy in high-purity YBCO crystals, which was attributed to the suppression of the thermally excited quasiparticles.[50]

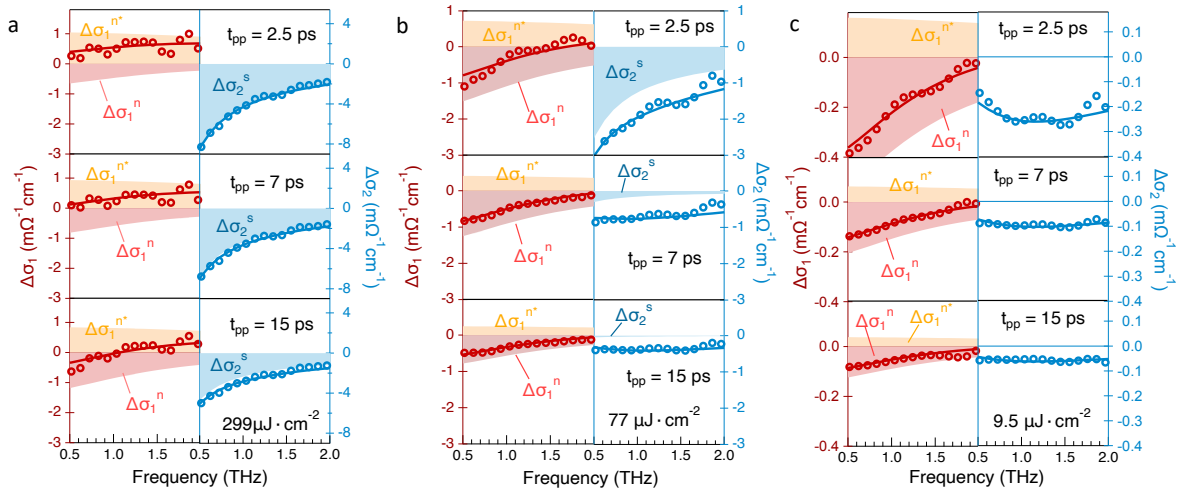


Figure 2. Pump-fluence dependence of photoinduced THz conductivities ($\Delta\tilde{\sigma}$). The real ($\Delta\sigma_1$) and imaginary ($\Delta\sigma_2$) parts of $\Delta\tilde{\sigma}$ for typical (a) high, (b) medium and (c) low pump fluences. The red and blue circles represent $\Delta\sigma_1$ and $\Delta\sigma_2$ recorded at indicated delays (t_{pp}), respectively. The measurements were performed at temperature of 3.4 K to minimize the thermal excitation of Cooper pairs. The pump photon energy is 1.55 eV. Solid curves are the fits based on Eq 2. The orange, red and blue shades represent the $\Delta\sigma_1^{n*}$, $\Delta\sigma_1^n$ and $\Delta\sigma_2^s$ (see main text for their definitions), respectively.

The steady-state THz conductivity shown above reveals the interplay between the superconducting and non-superconducting carriers (THz) under equilibrium condition, and their dynamics under nonequilibrium condition is investigated using transient THz spectroscopy. The experimental method is described in the Supplementary Material. Considering the coexistence of superconducting and non-superconducting carriers below T_c , nonequilibrium quasiparticles (QPs*) are generated either by destroying the superfluid or exciting the otherwise equilibrium quasiparticles (QPs⁰). Thus, the photoinduced change in $\tilde{\sigma}$ (denoted as $\Delta\tilde{\sigma}$) can be described by the following formula,

$$\Delta\tilde{\sigma} = -\Delta\rho_s \left(\frac{i}{\omega} \right) - \Delta\rho_n \left(\frac{\tau_n}{1 - i\omega\tau_n} \right) + (\Delta\rho_s + \Delta\rho_n) \left(\frac{\tau_n^*}{1 - i\omega\tau_n^*} \right) \quad (2)$$

where $\Delta\rho_n$ and $\Delta\rho_s$ are the photoinduced changes in $\rho_n(T)$ and $\rho_s(T)$, respectively, and τ_n^* is the scattering time of QPs*. The first and second terms on the right side of Eq. 2 account for a conductivity reduction due to the depopulation of the superfluid (denoted as $\Delta\sigma_s$) and QPs⁰, respectively, while the third term corresponds to a conductivity increase due to the photogenerated QPs*. As shown in Fig. 2, $\Delta\tilde{\sigma}$ at representative pump-THz delays (t_{pp}) exhibits strong dependence on the pump fluence (I_p). The extraction method of $\Delta\tilde{\sigma}$ is described in Supplementary Materials (Fig. S3). The measured $\Delta\tilde{\sigma}$ for different pump fluences can be simultaneously fitted by Eq. 2 (solid curves, Fig. 2) with common fitting parameters of τ_n and τ_n^* , revealing that the dependence of $\Delta\tilde{\sigma}$ on I_p or t_{pp} stems from the variation of $\Delta\rho_n$ and $\Delta\rho_s$. The value of τ_n is determined to be 0.12 ± 0.02 ps, consistent with that determined from the steady-state THz conductivity (Fig. 1e), and the value of τ_n^* is determined to be 0.034 ± 0.005 ps. We find that τ_n^* is much smaller than τ_n , implying that the mobility of QPs* should be lower than that of QPs⁰, in line with the literature.[51] By substituting the fitting parameters into Eq. 2, $\Delta\sigma_2^s$ (the imaginary part of the first term), $\Delta\sigma_1^n$ (the real part of the second term) and $\Delta\sigma_1^{n^*}$ (the real part of the third term) can be separately obtained (colored shades in Fig.2), which are exploited to trace the dynamics of the superfluid, QP⁰ and QP* components, respectively.

The optical excitation with a typical high I_p leads to a negative $\Delta\sigma_2$ with a nearly $1/\omega$ dependence and a small positive $\Delta\sigma_1$ (Fig. 2a) because of the depletion of superfluid and formation of QPs*.[19,20,36,45] The fitting reveals that $\Delta\sigma_1$ comprises a contribution from $\Delta\sigma_1^n$ with a negative value due to a reduction in the QP⁰ density after excitation. With increasing t_{pp} , $\Delta\sigma_2^s$ and $\Delta\sigma_1^{n^*}$ decay concurrently because QPs* condense into the superfluid (i.e., recovery of the superfluid), and this decay is accompanied by a growth of $\Delta\sigma_1^n$, indicating a continuous depletion of QPs⁰. As I_p drops to a lower level (Fig. 2b), $\Delta\sigma_2$ is initially dominated by $\Delta\sigma_2^s$ and then quickly evolves into a Drude response with increasing t_{pp} . The decay of $\Delta\sigma_2^s$ observed here is remarkably faster than that in the higher- I_p case, indicative of a quicker recovery of the superfluid density. On the contrary, the QP⁰ density recovers at a relatively slow pace, evidenced by the relatively slow decay of $\Delta\sigma_1^n$. When I_p falls into a typical low-fluence regime (Fig. 2c), both $\Delta\sigma_1$ and $\Delta\sigma_2$ resemble the Drude response, and

$\Delta\sigma_2^S$ can no longer be observed in $\Delta\sigma_2$ even at the short t_{pp} . The absence of $\Delta\sigma_2^S$ implies that the superfluid density remains intact after such a weak excitation, and the photoconductivity change solely arises from the excitation of QPs⁰. With increasing t_{pp} , the decay of $\Delta\sigma_1$ or $\Delta\sigma_2$ simply reflects the relaxation of QPs* into QPs⁰.

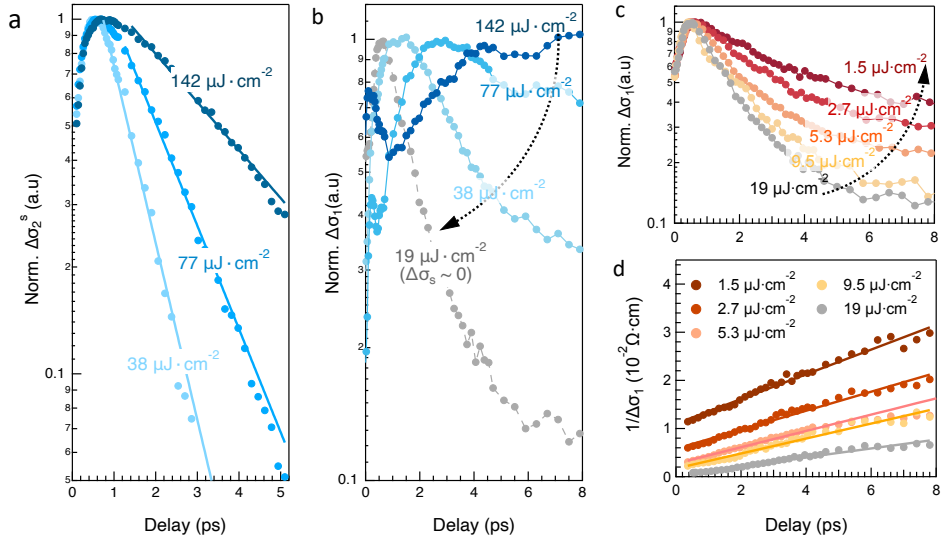


Figure 3. Recovery dynamics of superconducting and non-superconducting states after excitation. Normalized kinetics of (a) the superfluid component ($\Delta\sigma_2^S$) and (b) Drude component ($\Delta\sigma_1$) for typical high pump fluences. Note that the sign of the kinetics is changed after normalization. The lines in panel (a) are the monoexponential fits. The trace corresponding to $19 \mu\text{J} \cdot \text{cm}^2$ in panel (b) is plotted to illustrate the I_p -dependent decay rate, and under this pump fluence $\Delta\sigma_2^S$ is negligible. The dash curve with an arrow head is a visual aid for decreasing I_p . (c) Normalized $\Delta\sigma_1$ kinetics for the indicated pump fluences in the low- I_p regime. (d) The reciprocal of $\Delta\sigma_1$ ($1/\Delta\sigma_1$) plotted versus the delay time. The solid lines represent fits based on the biparticle annihilation model, and their slopes are equal to the rate constants. These kinetics were all measured at temperature of 3.4 K.

As demonstrated above, $\Delta\sigma_2^S$ only emerges when I_p exceeds a certain level at temperature well below T_c (e.g., 3.4 K). Above this critical I_p , the kinetics of $\Delta\sigma_2^S$ for different I_p are extracted through fitting $\Delta\tilde{\sigma}$ at different t_{pp} to explore the I_p -dependent superfluid recovery dynamics (Fig. 3a). In principle, these $\Delta\sigma_2^S$ kinetics should exhibit a biparticle decay pattern due to the pairwise condensation of QPs*, whereas they are well described by a single-exponential function with rate constant decreasing with increasing I_p . Similar experimental observation has been reported previously and interpreted by the Rothwarf-Taylor (R-T) model.[19,24,52,53] Although the R-T model

is originally derived for isotropic s-wave superconductors, it has also been widely exploited to deal with condensation dynamics of the nonequilibrium antinodal quasiparticles in d-wave superconductors.[19,24,52,53] In this model, pairing and pair breaking are mediated by high-frequency phonons (HFPs) with energy greater than the binding energy of the pairs, 2Δ (Δ is the superconducting energy gap), and the apparent decay of $\Delta\sigma_2^S$ kinetics is then masked by the relatively slow anharmonic decay of the nonthermal HFPs because a quasi-equilibrium is established between the QPs* and HFPs under high- I_p conditions.[19,24,36,52] Unlike the kinetics of $\Delta\sigma_2^S$, the kinetics of $\Delta\sigma_1$ (Fig. 3a) consist of a relatively slow growth component followed by a decay component, and both the growth and decay rates decrease with increasing I_p . The growth of $\Delta\sigma_1$ corresponds to an increase in the QP* density. However, this growth is accompanied by $\Delta\sigma_2^S$ decay, indicative of the recovery of the superfluid that should drain the QPs*. Considering that bosons (e.g., phonons) are released from condensation of QPs* into the superfluid, QPs⁰ that coexist with the superfluid can be excited by interacting with these nonthermal bosons so as to create extra QPs*. Therefore, the bosonic excitation of QPs⁰ probably accounts for the growth of $\Delta\sigma_1$ during the superconductivity recovery.

As demonstrated above, $\Delta\sigma_2^S$ is absent when I_p falls into the aforementioned low- I_p regime (Fig. 2c), suggesting that the superfluid density is intact under very weak excitation. In stark contrast with the high- I_p scenario, the kinetics of $\Delta\sigma_1$ in the low- I_p regime decays faster with increasing I_p (Fig. 3c), and the reciprocal of $\Delta\sigma_1$ kinetics ($1/\Delta\sigma_1$) displays a linear relationship with t_{pp} (Fig. 3d), a hallmark of the biparticle recombination pattern, which is well described by the following equation,

$$\frac{1}{\Delta\sigma_1(t_{pp})} = \frac{1}{\Delta\sigma_1(0)} + k_2 t_{pp} \quad (3)$$

where the slope, k_2 , is the rate constant for the biparticle decay. In the absence of $\Delta\sigma_2^S$, the kinetics of $\Delta\sigma_1$ (or $\Delta\sigma_2$) solely represents the dynamics of QPs*, so their biparticle decay pattern evidences that the QPs* return to the non-superconducting ground state (i.e., QPs⁰) through recombining into pairs. In other words, QPs⁰ may exist as pairs without long-range phase coherence (i.e., local pairs) at the temperature of 3.4 K. Thus, the very weak optical excitation breaks these local pairs rather than the superconducting pairs, leading to a reduction in both $\Delta\sigma_1$ and $\Delta\sigma_2$. The subsequent recovery represents the local pairing process, which is responsible for the biparticle decay of the $\Delta\sigma_1$ kinetics.

This pairwise recovering dynamics for the non-superconducting state are observed for optical pumps with wavelength ranging from ultraviolet to infrared (Fig. S4).

Because the superconducting energy gap is closed above T_c , the $\Delta\sigma_1$ kinetics measured at temperature above T_c reflects the intraband thermalization of QPs*. As shown in Fig. S5, the $\Delta\sigma_1$ kinetics measured above T_c indeed display a typical intraband thermalization character, including a fast component due to cooling via carrier-phonon interaction and a slow component due to heat dissipation. The cooling rate is independent of I_p , while the heat induced component becomes more significant with increasing I_p . Thus, the intraband relaxation of QPs* can be excluded as a probability to account for the $\Delta\sigma_1$ kinetics shown in Fig. 3d because of the distinctly different decay behaviors.

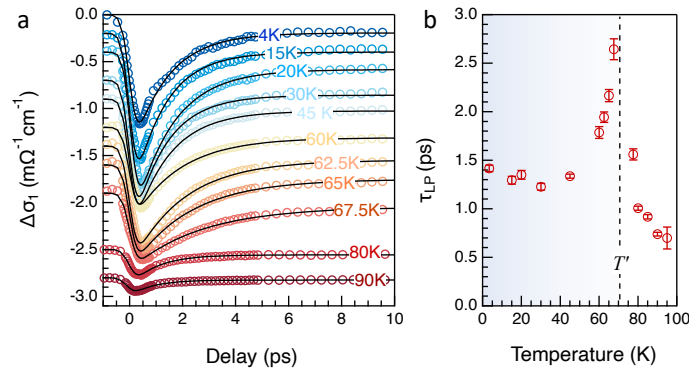


Figure 4. Temperature dependent recovery kinetics of the non-superconducting component. (a) Representative $\Delta\sigma_1$ kinetics in the low- I_p regime ($I_p = 9.1 \mu\text{J} \cdot \text{cm}^{-2}$) measured at indicated temperatures. (b) The plot of characteristic time (τ_{LP}) of the $\Delta\sigma_1$ decay versus temperature. The dash line indicates the divergence of τ_{LP} .

To examine the binding energy of the aforementioned local pairs, the local pairing dynamics represented by the $\Delta\sigma_1$ kinetics was measured at various temperatures below T_c . As shown in Fig. 4a, the decay rate of $\Delta\sigma_1$ kinetics first decelerates and then accelerates with increasing temperature below T_c . To more explicitly show this temperature-dependent decay trend, the $\Delta\sigma_1$ kinetics are fit by a biexponential function, and the characteristic time (τ_{LP}) corresponding to the fast decay component (also the major decay component) is plotted against temperature in Fig. 4b. The temperature dependent τ_{LP} exhibits a clear divergence near 70 K, coinciding with the phase

transition temperature shown in Fig. 1e. This critical temperature is denoted as T' . It is worth noting that these $\Delta\sigma_1$ kinetics exclusively measure the process that QPs* relax to the non-superconducting ground state (i.e., QP⁰ density recovery), whereas the divergent behavior near T' is reminiscent of the divergent behavior of quasiparticle condensation dynamics near T_c (i.e., superconducting state recovery) in optically excited cuprate superconductors.[26,39,45,54-56] Moreover, the temperature-dependent Δ in these superconductors is generally manifested as the characteristic divergence of the superfluid recovery time near T_c . [26,36,39,45,54-56] From a phenomenological perspective, the divergence of τ_{LP} for the local pairs near T' may also suggest a temperature-dependent collective energy gap (Δ'), and the binding energy of the local pairs is equal to $2\Delta'$. Thus, the divergence of τ_{LP} indicates that Δ' closes at temperature above T' , and then the individual quasiparticles rather than local pairs should dominate the non-superconducting state in the temperature interval of $T' < T < T_c$. Indeed, the decay rate of the $\Delta\sigma_1$ kinetics in this temperature interval is independent of the pump fluence, and their decay pattern resembles the intraband thermalization of QPs* (Fig. S6). The non-superconducting state tends to comprise more local pairs with decreasing temperature below T' . Thus, the decay rate of the $\Delta\sigma_1$ kinetics below T' becomes sensitive to the pump fluence, and a typical biparticle decay pattern appears when temperature is significantly lower than T' .

There are several signatures suggesting $\Delta' < \Delta$ below T' . First, T' is substantially lower than T_c . Second, the local pairs seem more vulnerable than the superconducting pairs because the former can be split with low I_p while the latter is intact, indicative of a smaller binding energy for the local pairs. Third, when both local and superconducting pairs are split, the recovery of the non-superconducting pairs is much slower than the recovery of the superconducting pairs (see Fig. 3c and 3d). Because the recovery time is inversely proportional to the energy gap,[24,39,54] the slower pairing for the local pairs implies that Δ' is probably smaller than Δ . Hence, we conjecture that Δ' should be smaller than Δ based on above observations.

We note that the local pairs below T' should be distinct from the preformed Cooper pairs that are generally discovered outside the superconducting dome (e.g., in the pseudogap regime) in cuprate superconductors. In striking contrast to the temperature-dependent local pairing observed here, the time constant for QPs* relaxation into preformed pairs is usually independent of

temperature.[24,39] Although it has been reported that Δ may coexist with a pseudogap below T_c , the characteristic time for quasiparticle pairing across the temperature-independent pseudogap is independent of the temperature.[39] Nevertheless, these local pairs share similarities with short-range PDW state observed in cuprates.[10,15,17,57] First, the PDW state was also found coexisting with the superconducting Cooper pairs at temperatures well below T_c . [9,13,15,58] Second, the PDW state also exhibits coherence on a length scale that is long enough to form an energy gap but is insufficiently long to sustain superfluidity.[15,17,57,59]

In summary, the dynamics of the non-superconducting state in optimally doped YBCO superconducting films were particularly interrogated using transient THz spectroscopy, which unveiled evidence for local pairs coexisting with superconducting pairs. As the superconducting gap arising from the long-range coherent pairing is generally manifested as a characteristic divergence of superconducting state recovery time near T_c , in this work, opening of an energy gap induced by local pairing with short-range coherence is invoked to interpret the temperature-dependent non-superconducting pairs recovery dynamics and the clear divergence of the recovery time near 70 K (remarkably lower than T_c). To explore the phase diagram for local pairs below T_c , extending the investigation of the temperature-dependent local pairing dynamics to cuprates with various hole doping densities is motivated as further work.

Acknowledgements. Y.Y. acknowledges the National Natural Science Foundation of China under Grant Nos. 22175145, National Key Research and Development Program of China (2022YFB3803304), Fundamental Research Funds for the Central Universities under Grant number 20720220011 and 20720240150.

Reference:

- [1] D. J. Scalapino, Rev. Mod. Phys. **84**, 1383 (2012).
- [2] B. Keimer, S. A. Kivelson, M. R. Norman, S. Uchida, and J. Zaanen, Nature **518**, 179 (2015).
- [3] T. Dubouchet, B. Sacépé, J. Seidemann, D. Shahar, M. Sanquer, and C. Chapelier, Nat. Phys. **15**, 233 (2019).
- [4] K. M. Bastiaans, D. Chatzopoulos, J.-F. Ge, D. Cho, W. O. Tromp, J. M. van Ruitenbeek, M. H. Fischer, P. J. de Visser, D. J. Thoen, E. F. C. Driessen, T. M. Klapwijk, and M. P. Allan, Science **374**, 608 (2021).
- [5] B. L. Kang, M. Z. Shi, S. J. Li, H. H. Wang, Q. Zhang, D. Zhao, J. Li, D. W. Song, L. X. Zheng, L. P. Nie, T. Wu, and X. H. Chen, Phys. Rev. Lett. **125**, 097003 (2020).

- [6] P. M. C. Rourke, I. Mouzopoulou, X. Xu, C. Panagopoulos, Y. Wang, B. Vignolle, C. Proust, E. V. Kurganova, U. Zeitler, Y. Tanabe, T. Adachi, Y. Koike, and N. E. Hussey, *Nat. Phys.* **7**, 455 (2011).
- [7] P. Zhou, L. Chen, Y. Liu, I. Sochnikov, A. T. Bollinger, M.-G. Han, Y. Zhu, X. He, I. Božović, and D. Natelson, *Nature* **572**, 493 (2019).
- [8] H. B. Yang, J. D. Rameau, P. D. Johnson, T. Valla, A. Tselik, and G. D. Gu, *Nature* **456**, 77 (2008).
- [9] S. Ye, C. Zou, H. Yan, Y. Ji, M. Xu, Z. Dong, Y. Chen, X. Zhou, and Y. Wang, *Nat. Phys.* **19**, 1301 (2023).
- [10] X. Li, C. Zou, Y. Ding, H. Yan, S. Ye, H. Li, Z. Hao, L. Zhao, X. Zhou, and Y. Wang, *Phys. Rev. X* **11**, 011007 (2021).
- [11] W. Ruan, X. Li, C. Hu, Z. Hao, H. Li, P. Cai, X. Zhou, D.-H. Lee, and Y. Wang, *Nat. Phys.* **14**, 1178 (2018).
- [12] H. Li, H. Li, Z. Wang, S. Wan, H. Yang, and H.-H. Wen, *NPJ Quantum Mater.* **8**, 18 (2023).
- [13] M. H. Hamidian, S. D. Edkins, S. H. Joo, A. Kostin, H. Eisaki, S. Uchida, M. J. Lawler, E. A. Kim, A. P. Mackenzie, K. Fujita, J. Lee, and J. C. S. Davis, *Nature* **532**, 343 (2016).
- [14] S. D. Edkins, A. Kostin, K. Fujita, A. P. Mackenzie, H. Eisaki, S. Uchida, S. Sachdev, M. J. Lawler, E.-A. Kim, J. C. Séamus Davis, and M. H. Hamidian, *Science* **364**, 976 (2019).
- [15] P. Choubey, S. H. Joo, K. Fujita, Z. Du, S. D. Edkins, M. H. Hamidian, H. Eisaki, S. Uchida, A. P. Mackenzie, J. Lee, J. C. S. Davis, and P. J. Hirschfeld, *Proc. Natl Acad. Sci. USA* **117**, 14805 (2020).
- [16] Z. Du, H. Li, S. H. Joo, E. P. Donoway, J. Lee, J. C. S. Davis, G. Gu, P. D. Johnson, and K. Fujita, *Nature* **580**, 65 (2020).
- [17] C. Setty, L. Fanfarillo, and P. J. Hirschfeld, *Nat. Commun.* **14**, 3181 (2023).
- [18] Y. Liu, T. Wei, G. He, Y. Zhang, Z. Wang, and J. Wang, *Nature* **618**, 934 (2023).
- [19] R. A. Kaindl, M. A. Carnahan, D. S. Chemla, S. Oh, and J. N. Eckstein, *Phys. Rev. B* **72**, 060510 (2005).
- [20] B. Cheng, D. Cheng, K. Lee, L. Luo, Z. Chen, Y. Lee, B. Y. Wang, M. Mootz, I. E. Perakis, Z.-X. Shen, H. Y. Hwang, and J. Wang, *Nat. Mater.* (2024).
- [21] Y. Toda, S. Tsuchiya, M. Oda, T. Kurosawa, S. Katsumata, M. Naseska, T. Mertelj, and D. Mihailovic, *Phys. Rev. B* **104**, 094507 (2021).
- [22] I. M. Vishik, F. Mahmood, Z. Alpichshev, N. Gedik, J. Higgins, and R. L. Greene, *Phys. Rev. B* **95**, 115125 (2017).
- [23] C. R. Hunt, D. Nicoletti, S. Kaiser, D. Pröpper, T. Loew, J. Porras, B. Keimer, and A. Cavalleri, *Phys. Rev. B* **94**, 224303 (2016).
- [24] C. Giannetti, M. Capone, D. Fausti, M. Fabrizio, F. Parmigiani, and D. Mihailovic, *Adv. Phys.* **65**, 58 (2016).
- [25] L. Perfetti, B. Sciollo, G. Biroli, C. J. van der Beek, C. Piovera, M. Wolf, and T. Kampfrath, *Phys. Rev. Lett.* **114**, 067003 (2015).
- [26] S. G. Han, Z. V. Vardeny, K. S. Wong, O. G. Symko, and G. Koren, *Phys. Rev. Lett.* **65**, 2708 (1990).
- [27] Y. Xiao, J. Wu, J. I. Dadap, K. M. Awan, D. Yang, J. Liang, K. Watanabe, T. Taniguchi, M. Zonno, M. Bluschke, H. Eisaki, M. Greven, A. Damascelli, and Z. Ye, *Nano Lett.* (2024).
- [28] G. P. Segre, N. Gedik, J. Orenstein, D. A. Bonn, R. Liang, and W. N. Hardy, *Phys. Rev. Lett.* **88**, 137001 (2002).
- [29] P. Kusar, V. V. Kabanov, J. Demsar, T. Mertelj, S. Sugai, and D. Mihailovic, *Phys. Rev. Lett.* **101**,

227001 (2008).

- [30] T. Dong, S.-J. Zhang, and N.-L. Wang, *Adv. Mater.* **35**, 2110068 (2023).
- [31] J. C. Petersen, A. Farahani, D. G. Sahota, R. Liang, and J. S. Dodge, *Phys. Rev. B* **96**, 115133 (2017).
- [32] J. Orenstein and J. S. Dodge, *Phys. Rev. B* **92**, 134507 (2015).
- [33] M. Beyer, D. Städter, M. Beck, H. Schäfer, V. V. Kabanov, G. Logvenov, I. Bozovic, G. Koren, and J. Demsar, *Phys. Rev. B* **83**, 214515 (2011).
- [34] A. Pashkin, M. Porer, M. Beyer, K. W. Kim, A. Dubroka, C. Bernhard, X. Yao, Y. Dagan, R. Hackl, A. Erb, J. Demsar, R. Huber, and A. Leitenstorfer, *Phys. Rev. Lett.* **105**, 067001 (2010).
- [35] D. Fausti, R. I. Tobey, N. Dean, S. Kaiser, A. Dienst, M. C. Hoffmann, S. Pyon, T. Takayama, H. Takagi, and A. Cavalleri, *Science* **331**, 189 (2011).
- [36] J. Demsar, R. D. Averitt, A. J. Taylor, V. V. Kabanov, W. N. Kang, H. J. Kim, E. M. Choi, and S. I. Lee, *Phys. Rev. Lett.* **91**, 267002 (2003).
- [37] H. Jang, S. Song, T. Kihara, Y. Liu, S.-J. Lee, S.-Y. Park *et al.*, *Sci. Adv.* **8**, eabk0832 (2022).
- [38] J. Graf, C. Jozwiak, C. L. Smallwood, H. Eisaki, R. A. Kaindl, D. H. Lee, and A. Lanzara, *Nat. Phys.* **7**, 805 (2011).
- [39] J. Demsar, B. Podobnik, V. V. Kabanov, T. Wolf, and D. Mihailovic, *Phys. Rev. Lett.* **82**, 4918 (1999).
- [40] D. H. Torchinsky, G. F. Chen, J. L. Luo, N. L. Wang, and N. Gedik, *Phys. Rev. Lett.* **105**, 027005 (2010).
- [41] S. J. Zhang, Z. X. Wang, H. Xiang, X. Yao, Q. M. Liu, L. Y. Shi, T. Lin, T. Dong, D. Wu, and N. L. Wang, *Phys. Rev. X* **10**, 011056 (2020).
- [42] F. Mahmood, X. He, I. Božović, and N. P. Armitage, *Phys. Rev. Lett.* **122**, 027003 (2019).
- [43] L. S. Bilbro, R. V. Aguilar, G. Logvenov, O. Pelleg, I. Božović, and N. P. Armitage, *Nat. Phys.* **7**, 298 (2011).
- [44] L. S. Bilbro, R. Valdés Aguilar, G. Logvenov, I. Bozovic, and N. P. Armitage, *Phys. Rev. B* **84**, 100511 (2011).
- [45] R. D. Averitt, G. Rodriguez, A. I. Lobad, J. L. W. Siders, S. A. Trugman, and A. J. Taylor, *Phys. Rev. B* **63**, 140502 (2001).
- [46] M. C. Nuss, P. M. Mankiewich, M. L. O'Malley, E. H. Westerwick, and P. B. Littlewood, *Phys. Rev. Lett.* **66**, 3305 (1991).
- [47] R. D. Averitt, G. Rodriguez, J. L. W. Siders, S. A. Trugman, and A. J. Taylor, *J. Opt. Soc. Am. B* **17**, 327 (2000).
- [48] S. D. Brorson, R. Buhleier, I. E. Trofimov, J. O. White, C. Ludwig, F. F. Balakirev, H. U. Habermeier, and J. Kuhl, *J. Opt. Soc. Am. B* **13**, 1979 (1996).
- [49] M. Prohammer and J. P. Carbotte, *Phys. Rev. B* **43**, 5370 (1991).
- [50] A. Hosseini, R. Harris, S. Kamal, P. Dosanjh, J. Preston, R. Liang, W. N. Hardy, and D. A. Bonn, *Phys. Rev. B* **60**, 1349 (1999).
- [51] N. Gedik, J. Orenstein, R. Liang, D. A. Bonn, and W. N. Hardy, *Science* **300**, 1410 (2003).
- [52] V. V. Kabanov, J. Demsar, and D. Mihailovic, *Phys. Rev. Lett.* **95**, 147002 (2005).
- [53] A. Rothwarf and B. N. Taylor, *Phys. Rev. Lett.* **19**, 27 (1967).
- [54] V. V. Kabanov, J. Demsar, B. Podobnik, and D. Mihailovic, *Phys. Rev. B* **59**, 1497 (1999).

- [55] D. Dvorsek, V. V. Kabanov, J. Demsar, S. M. Kazakov, J. Karpinski, and D. Mihailovic, *Phys. Rev. B* **66**, 020510 (2002).
- [56] Y. H. Liu, Y. Toda, K. Shimatake, N. Momono, M. Oda, and M. Ido, *Phys. Rev. Lett.* **101**, 137003 (2008).
- [57] D. F. Agterberg, J. C. S. Davis, S. D. Edkins, E. Fradkin, D. J. Van Harlingen, S. A. Kivelson, P. A. Lee, L. Radzihovsky, J. M. Tranquada, and Y. Wang, *Annu. Rev. Condens. Matter Phys.* **11**, 231 (2020).
- [58] S. Wang, P. Choubey, Y. X. Chong, W. Chen, W. Ren, H. Eisaki, S. Uchida, P. J. Hirschfeld, and J. C. S. Davis, *Nat. Commun.* **12**, 6087 (2021).
- [59] Z. Dai, T. Senthil, and P. A. Lee, *Phys. Rev. B* **101**, 064502 (2020).